Detection and characterization of Levy flights in chaotic advection phenomena

B. RICAUD*

*Laboratoire d'Analyse, Topologie, Probabilité, AMU,
Marseille, France
E-mail: bricaud@cmi.univ-mrs.fr

F. BRIOLLE

*Centre de Physique Théorique   &   CReA, BA 701
Marseille, France   Salon, France
E-mail: briolle@cpt.univ-mrs.fr*

X. LEONCINI

*Centre de Physique Théorique,
Marseille, France
E-mail: xavier.leoncini@cpt.univ-mrs.fr*

Transport of advected passive particles in two dimensional flows with coherent structures (vortex) is anomalous when it contains Levy flights. We suggest a method for detecting these Levy flights in the signals, allowing to characterize the transport (diffusive or anomalous). We use time-frequency techniques such as Fractional Fourier transform and matching pursuit in order to be robust to noise.

Keywords: Levy flights, anomalous transport, fractional Fourier transform, signal analysis.

1. Introduction

In order to analyse chaotic transport phenomena and quantify anomalous transport, several tools are being used in the nonlinear physics community such as a fractal analysis of the trajectories[], giving Lyapunov exponents, multifractal analysis [?], or statistical analysis [?] and analysis of long-tailed probability density functions of polynomial decrease. In this article, we suggest a new method for analysing a particular case of anomalous transport. In this special case, the particles involved in the transport encounter typi-

2

cally short periods of balistic transport (Lévy flights) in between standard random walks (Brownian motion). From a statistical point of view, this is a anomalous transport phenomenon and this anormality can be estimated by the usual techniques to obtain one or several global estimators. But it can be caracterized in a more accurate way by detecting and counting the amount and duration of these levy flights. Moreover, in the case of real data (not simulations), noise is present in the signal to analyze. The standard methods fail to discriminate the statistical behavior of the signal from the one of the noise. Our signal processing analysis is able to detect and extract levy flights even embedded in noise (of reasonable amplitude). This is definitively an asset in view of using it on practical applications.

The signal processing method relies on the use of the uncertainty principle. This principle states that time and frequency (momentum and position in quantum mechanics) cannot be known simultaneously with arbitrary precision. If we call Δt the accuracy of the measure in time and Δf the accuracy in frequency, the Heisenberg principle states that:

$$\Delta t \cdot \Delta f \geq c,$$

where c is a strictly positive constant. This phenomenon is usually seen as a problem and large efforts have been done to minimize uncertainty. However, in the present work we are taking advantage of it. Indeed, we propose to transfer the tracer trajectory seen as a signal to the time-frequency plane: the Brownian motion becomes a fuzzy stain whereas the levy flights remain relatively sharp. The detection of Lévy flights turns into the detection of straight lines in the time-frequency plane, something which can be efficiently done with the Fractional Fourier transform. The uncertainty principle gives to our detection algorithm the ability to accurately detect flights even in the presence of noise. Moreover, it can be implemented in a fast manner relying on the fast Fourier transform: the complexity is of $\mathcal{O}(N^2 \log N)$, where N is the size of the sampled signal giving the advection of one particle.

In part 2 we present the physical problem which motivated the establishment of our new signal processing technique. The notion of transport and Lévy flight is stated with precision along with the type of data to analyze. In part 3 the method for analyzing this particular anomalous transport is described in details. It is illustrated with its application to data from part 2, the results of the detection of Lévy flights are presented at the end.

2. Chaotic advection phenomena

In this section we introduce the phenomenon of stickiness that occurs in low-dimensional Hamiltonian systems, for this purpose we consider sepcifically the phenomenon of chaotic advection of passive tracers in a flow generated by three vortices.

2.1. *Definitions*

We consider the flow $\mathbf{v}(\mathbf{r}, t)$ of an incompressible fluid ($\nabla \cdot \mathbf{v} = 0$). A particle can be considered a passive particle if once it is placed in the fluid, its presence has no impact on the flow itself. In this setting the trajectories of the passive particle can be deduced directly from the flow, since the speed of the passive particle is identical to the one of the fluid itself. The motion is then a solution of the following differential equation:

$$\dot{\mathbf{r}} = \mathbf{v}(\mathbf{r}, t) , \tag{1}$$

where $\mathbf{r} = (x, y, z)$ corresponds to the passive particle position. If we consider a two-dimensional flow the motion can be cast in a Hamilotnioan formalism. Indeed, we have $\nabla \cdot \mathbf{v} = 0$, thus up to some gradient a stream function $\mathbf{\Psi}$ can be defined such that $\mathbf{v} = \nabla \wedge \mathbf{\Psi}$, and in a two-dimensional case, $\mathbf{\Psi} = \Psi \, \mathbf{z}$ resumes to a scalar field Ψ, $\mathbf{z}$ being the unit vector perpendiculare to the two dimensional plane. In this setting Eq. (1) become

$$\dot{x} = \frac{\partial \Psi}{\partial y}, \qquad \dot{y} = -\frac{\partial \Psi}{\partial x} . \tag{2}$$

We shall notice that the couple (x, y) corresponds either to the canonical conjugate variables of the Hamiltonian Ψ. We have obtain a one dimensional integrable Hamiltonian system if Ψ is independent of time, stating the simple fact that particles follow stream lines. If Ψ depends on time, we generically obtain Hamiltonian chaos and a system with $1 - \frac{1}{2}$ degree of freedom. This chaotic nature of the trajectories is in this context referred to the phenomenon of Chaotic advection. Indeed even if the flow has a laminar (non turbulent structure), passive particles or tracers have chaotic trajectories.[?,?,?] As a consequence mixing is considerably enhanced in chaotic regions of the flow, in the sense that chaotic motions mixes much faster than molecular diffusion.[?,?,?] This phenomenon is of crucial importance when dealing with mixing in micro-fluidic devices, as Reynolds number are usually small and chaotic mixing becomes, de facto, the preferred tool. there are moreover a multitude of physical systems and applications dsipalying such chaotic motion for instance in geophysical flows or magnetized fusion

4

plasmas.[?,?,?,?,?,?,?,?,?] To generate the flows from which we will analyze the data we consider flows generated by a system with three point vortices.

2.2. *A system of point vortices*

In order tpo describe a system of point vortices, it is best to start with the Euler equation for the vorticity in a two-dimensional incompressible flow:

$$\frac{\partial \Omega}{\partial t} + [\Omega, \Psi] = 0 \,, \; \Omega = -\nabla^2 \Psi \,, \tag{3}$$

where $[\cdot, \cdot]$ and denotes the Poisson brackets. We now consider a vorticity field given by a superposition of Dirac functions:

$$\Omega(\mathbf{r}, t) = \sum_{i=1}^{N} k_i \delta\left(\mathbf{r} - \mathbf{r}_i(t)\right) \,. \tag{4}$$

Here, k_i designate the vorticity of the point vortex localized at point $\mathbf{r}_i(t)$. This point vortex distribution is a solution of the Euler equation if the N positions of the vortices $\mathbf{x}_i(t)$ have a specific dynamics.[?] In fact the dynamics of the vortices corresponds to N-body Hamiltonian dynamics and when the flow is considered on the plane, the Hamiltonian writes

$$H = \frac{1}{2\pi} \sum_{i>j} k_i k_j \ln |\mathbf{r}_i - \mathbf{r}_j| \,, \tag{5}$$

where $k_i y_i$ and x_i are the canonically conjugate variables of the Hamiltonian (5) and locate the position $\mathbf{r}_i(t)$ in the plane.

The vortex motion resulting from Hamiltonian (5) just states that each vortex is advected by the velocity field generated by the other vortices. We then also have access to the stream function which acts as the Hamiltonian of the passive tracers

$$\Psi(\mathbf{r}, t) = -\frac{1}{2\pi} \sum_{i=1}^{N} k_i \ln |\mathbf{r} - \mathbf{r}_i(t)| \,. \tag{6}$$

Before moving on, we notice that the Hamiltonian (5) is invariant by translation and by rotation in the plane. Given this, it can be shown the system is integrable if the number of point vortices N is such that $N \leq 3$, on the other hand vortex motion is not integrable and consequently chaotic if $N > 3$.[?,?] In order to generate a laminar time-dependent flow we consider the flow generated by three vortices.

Also since we are interested in asymptotic transport properties we have considered a periodic motion of the vortices. Work related to transport for
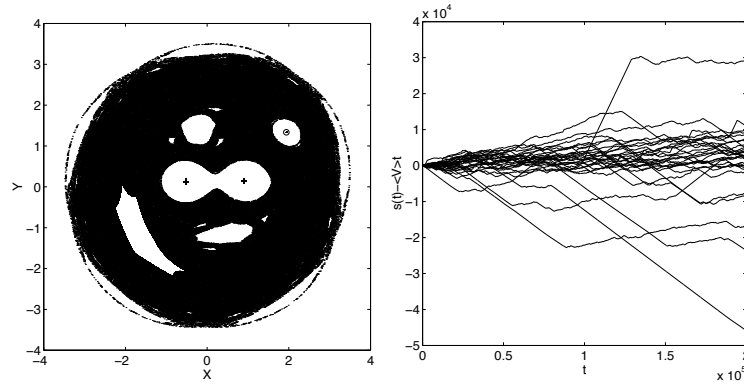
Fig. 1.   Left: Poincaré section of a system of three point vortices. Vorticities are $(-0.2, 1, 1)$. Right: Deviation from average arc-length $(s(t) - Vt)$ versus time for an ensemble of 30 particles advected in the flow. We notice the presence of Lvy flights. The run is performed over 20000 (quasi-)periods of the vortex motion.

the case of three identical vortices can be found in.[?,?] Here we want to have vortices of different signs and check the influence on transport of the finite time singularity

2.3. *Stickiness and anomalous transport*

We just have discussed chaotic mixing in a flow generated by three point vortices. In fact transport in a complex system can be anomalous. To be more precise in the nomenclature, there exist classification of the type of transport based on the value of the characteristic exponent of the evolution of the second moment.

Transport is said to be anomalous if it is not diffusive in the sense $\langle X^2 \rangle \sim t^\mu$, $\mu \neq 1$

(1) If $\mu < 1$ transport is anomalous and one refers to it as sub-diffusion
(2) If $\mu = 1$ transport is Gaussian and one refers to it as diffusion
(3) If $\mu > 1$ transport is anomalous and one refers to it as super-diffusion

When considering system of three point vortices, as the one depicted in Fig. 1, one notices that the chaotic sea is finite. Moreover, transport properties are quite obvious when we are within an island of stability where motion is regular, thus we are interested in transport properties resulting from trajectories living in the chaotic sea which results from chaotic advection. Since the sea is bounded, it is not convenient to consider transport for

6

long times based on particle positions (the sea being filled quite fast). We are thus considering transport properties based on the length of trajectories and measure the curvilinear arc-length, and the transport and dispersion associated to this quantity

$$s_i(t) = \int_0^t |v_i(\tau)|d\tau \,, \tag{7}$$

where $v_i(\tau)$ is the speed of particle i at time τ. Then to characterize and study transport we compute the moments

$$M_q(t) \equiv \langle |s(t) - \langle s(t) \rangle|^q \rangle \,, \tag{8}$$

where $\langle \dots \rangle$ corresponds to ensemble averaging over different trajectories. In fact since the the ergodic measure may not be uniform, in order to sample it properly it is best to consider different portions of length t of trajectories computed for a long time, rather than a large number of initial conditions computed for "short" times, $i.$ $e.$ when dealing with numerics it is best to have a strong processor, rather than a parrallel computer. From teh evolution of the different moments, we we get a characteristic exponent

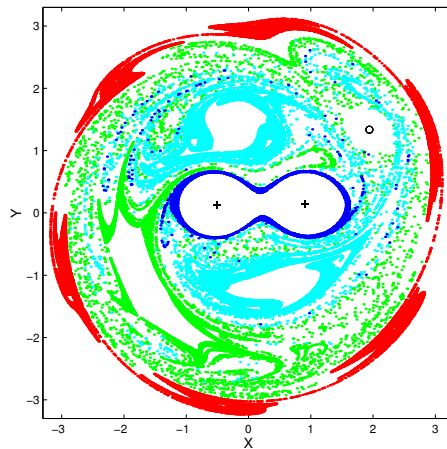$$M_q(t) \sim t^{\mu(q)} \,. \tag{9}$$

Fig. 2.   Localization of the regions contributing to the type of flights depicted in Fig. 1.

It was shown that for the point vortex flow, the transport is superdiffusive and multi-fractal.[?] These anamalous features were traced back to the phenomenon of stickiness: when a trajectory arrives in the neighbourhood of an island of stability it can get stuck around the island for arbitrary large times which act as pseudo-traps. This generates strong memory effects (slow decay of correlations) and as a consequence displays anomalous transport properties. In Fig. 2, the sticky region are identified (see[?] for details). Once a trajectory gets stuck around an island after a transient its length grows almost linearly with time, with a speed generically different then the ensemble average one, which translates in the presence of Lvy flights. We have drawn in Fig. **??** the relative evolution of the length with respect to the mean of an ensemble of 30 different particles. Indeed One can see that the time evolution is reminiscent of some random walks by parts coming from the chaotic sea and there are some parts where the evolution looks regular and ballistic usually referred to as Levy flights, each different slope corresponding to a different sticky region (Fig. 2).

3. Time-frequency technique

We shall now introduce the particularities of the data set from a signal processing point of view and describe the analysing technique. For clarity, the result of each step will be illustrated with applications to the simulated data of the previous part (trajectories of tracers evolving in the flow generated by three vortices).

3.1. *The data set*

A typical trajectory s is a one-dimensional signal of $N = 1000$ sampling points $s(t)$, $t \in [1, N]$. An example of such signal is shown on Fig. 3 (left) and a set of trajectories on Fig. 1 (right). Several parts can be distinguished: a random fluctuation (Brownian motion) and some *almost* linear segments of different length corresponding to Lévy flights. Our technique is dedicated to the detection these linear parts and the measure of their length and slope.

3.2. *The detection method*

As illustrated in Fig. 1 (right) and Fig. 3 (left), Lévy flights correspond to an almost linear evolution of the arclength. It is then important to notice that due to the uncertainty principle:

- random fluctuations in frequency cannot be rendered precisely in the

8

time-frequency plane. It requires to be precise both in time and frequency, which is forbidden.

- linear parts or more generally slowly varying frequency components are emphazised by the time-frequency representation. Moreover, linear parts, called chirp signals, can be detected efficiently using the fractional Fourier transform.

It is then interesting and natural to us to take advantage of this fact for the analysis of the data set. To perform our analysis we shall therefore interpret the arclength $s(t)$ as the phase derivative (the fluctuation of the "frequency component") of a new signal $S(t)$. This corresponds to the first step of the process: Let us introduce the phase

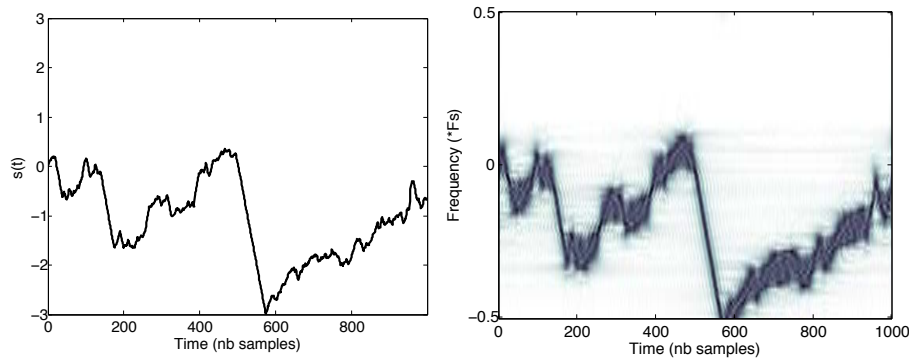$$\varphi(t) = \sum_{\tau=1}^{t} s(\tau), \tag{10}$$

and the signal

Fig. 3.   Left:Length of a single particle. Right: Short-time Fourier transform of S.

$$S(t) = e^{i\varphi(t)}. \tag{11}$$

The above signal is a non-stationary signal of magnitude one and made of a single frequency component which fluctuations are the one of the initial function $s(t)$. To better understand what it means, the time-frequency representation of S has been drawn on Fig. 3 (right). It is also called the spectrogram[1] and it is the absolute value of the short-time Fourier transform of S. One single frequency component can be seen which mimick the behavior of the signal s plotted on the right. But the important difference

9

is now, because of the uncertainty principle, that brownian fluctuations become diffuse stains in Fig. 3 (right). As a consequence pure random behavior is blurred, but linear parts remain sharp. Our first objective is attained: le linear behavior has been emphazised over the brownian motion, thanks to the uncertainty principle.

We now move on to the second part of the process. We search for lines in the time-frequency 'picture'. For this purpose we project the signal $S(t)$ on several orthogonal basis of chirps signals. Given a parameter $\theta \in (-\pi, \pi)$, we introduce the basis of chirps $\{\psi_{\theta,\mu}\}_\mu$ with a frequency slope of $\frac{1}{\tan \theta}$,

$$\psi_{\theta,\mu}(t) = e^{i(\frac{1}{2\tan \theta} t^2 + \frac{\mu}{\sin \theta} t)}. \tag{12}$$

Since $t \in [1, N]$, $\mu = 2\pi n/N$ with $n \in [1, N]$. Notice that $\mu/\sin \theta$ is the frequency value at $t = 0$ (frequency offset) of the chirp $\psi_{\theta,\mu}$. The projection of the signal is described by the following procedure and it is equivalent[2] to applying the Fractional Fourier transform (up to a normalizing factor):

$$C(\theta, \mu) = \sum_{t=1}^{N} S(t)\overline{\psi_{\theta,\mu}(t)}, \tag{13}$$

where the bar denotes the complex conjugate. Since Lévy flights may have different slopes, it is necessary to project onto several basis of chirps, each one having a different θ. Several θ ($M = N$ values between $(-\pi)$ and π) are chosen for the projection giving the $M \times N$ matrix $C(\theta, \mu)$. When the characteristics of a chirp (frequency slope and offset) match the one of a "frequential picture"-Lévy flight present in the signal, a peak is obtained for $|C|$. The amplitude of this peak is directly proportional to the length of the flight.

Taking the signal shown in Fig. 3 as an example, there is a specific direction θ_m (related to the slope of the largest Levy flight) where a peak in localized in the row $|C(\theta_m, \cdot)|$, as illustrated in Fig. 4. For $\mu_m \sim 420$, the sharp peak $|C(\theta_m, \mu_m)|$ gives evidence that there is a Lévy flight with a particular slope $\frac{1}{\tan \theta_m}$, with a length proportional to $|C(\theta_m, \mu_m)|$. This search for maxima is the process that detects linear parts in the time-frequency plane.

Once the first maximum is identified, we can make several choices. The simplest one is to look for the second highest peak, third and so on until the amplitude of the n-th peak detected reaches a chosen threshold. The output of the algorithm gives a set of n values for θ (slopes) and for $|C(\theta, \mu)|$ (lengths). This finishes the analysis of one particle trajectory.
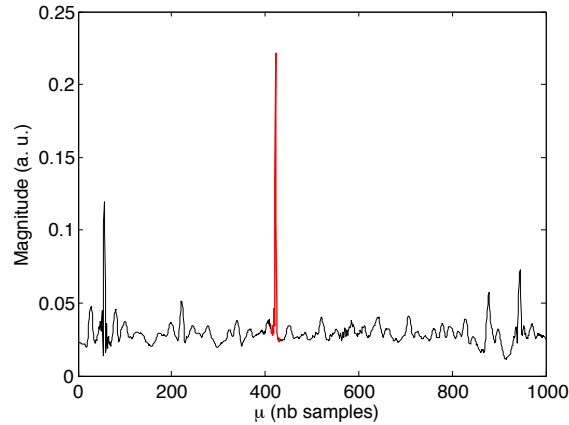
10

Fig. 4.   For θ_m, signal projections $|C(\theta_m, \mu)|$.

The second choice is more complex but potentially more interesting. Since we have projected S onto a orthogonal basis, we can set the detected peak at θ_m, μ_m to zero and reconstruct a signal S_1 by calculating:

$$S_1 = S - C(\theta_m, \mu_m)\psi_{\theta_m, \mu_m}.$$

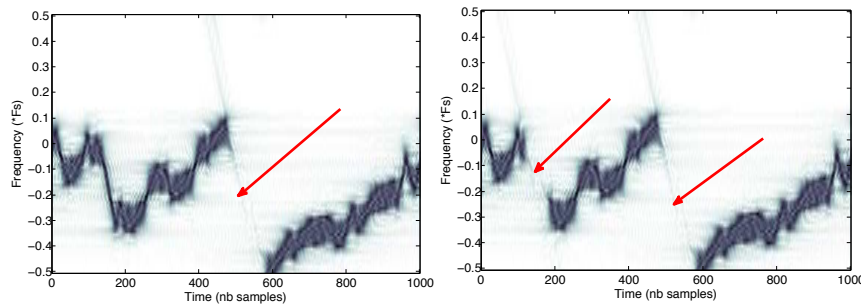This step is illustrated in Fig. 5 (left), which represents the short-time

Fig. 5.   Short-time Fourier transform of the signal S_1 and S_2. Left : the longest Lévy flight have been removed. Right : two Lévy flights have been removed.

Fourier transform of the newly recreated signal S_1. The largest frequency slope of S has been completely removed, the rest remaining untouched. This shows the efficiency of our method. The signal S_1 can then be processed similarly to S, i.e. projecting on chirp bases, finding the maximum and taking it out, to lead to a new signal S_2 where the second longest linear part

has been removed, Fig. 5 (right). Again, one clearly sees the efficiency of the algorithm. Indeed, in this example, after two iterations of the process we managed to remove the two longest Lévy flights. This iterative process leading to $S_1, S_2, \cdots, S_n$ is the principe of the matching pursuit[4] decomposition of a signal. The advantage of this method is that the random part of the signal is not affected by the decomposition and this allow for future analyses of the random part without the flights (in the time-frequency picture).

The steps of the process can be summarized as follow :

- Trajectory as a phase derivative of a signal $S(t)$: time-frequency transformation
- Search for lines in the time-frequency 'picture' : projection on a basis of chirps
- Lévy flight detection : peak picking on the matrix C and matching pursuit.

Remark 1: The computational complexity for obtaining the matrix C is of order $N^2 \log N$. For each θ the projection onto the chirp basis is performed via a fast Fourier transform[2,3] of complexity $N \log N$. This is done for a number of θ proportional to N.

Remark 2: For Lévy flights with steep slopes, numerical problems may arise due to the discretization. The solution used here is to make a 90 degrees rotation of the signal in the time-frequency plane before the projection on chirps and adapt the values of θ in consequence: this rotation is simply obtained by applying a Fourier transform to the signal S.

3.3. *Robustness to noise*

3.4. *Blind characterization of Lévy flights in the advected data*

As a test of the method we now consider the data obtained from the advection of 253 tracers in the point vortex flow described in section 1. Our goal is to detect the multi-fractal nature of the transport resulting from the sticky islands, which would serve as a proof of concept and pave the way to apply the method to numerical and experimental data.

12

4. Conclusions

The first step of the method help emphasing the straight lines over random fluctuations.

The second step consists in the detection of straight lines in the time-frequency image. The Fractional Fourier transform applied to a one-variable signal is similar to a Radon transform or Hough transform of a standard image.

This method and its first results open the way to more systematic detections of Levy flights in anomalous transport phenomena. The detection algorithm is efficient and fast, allowing the analysis of a large number of tracers trajectories in a short time. The output, yielding the number Levy flight and their duration, can be analysed in a second step by statistical tools (e.g. mean number of flight in a trajectory, mean length, variance,...). This will lead to a more accurate characterization of this particular case of anomalous transport.

Open Questions

- How to analyse other coherent shapes in the signal (more complex than linear)?
- Can we analyse the remaining random signal S_n and recover brownian motion?
- This method can detect noisy flights, what is the maximal level of noise admitted?
- What is the minimal length of a Levy flight?
- Is it possible to quantify anomalous transport with this technique?

5. acknowledgements

References

1. Flandrin P., Temps-Fréquence, Hermès, 1993-1998.
2. Almeida L. B., The fractional Fourier transform and time-frequency representations, IEEE Trans. Sig. Processing 42 (11), 3084-3091 (1994).
3. F. Clairet, B. Ricaud, F. Briolle, S. Heuraux, C. Bottereau, New signal processing technique for density profile reconstruction using reflectometry, Rev. Sci. Instrum. 82, 8 (2011), 9p.
4. Mallat S., Zhang Z., Matching pursuits with time-frequency dictionnaries. IEEE Trans. Sig. Processing, 41(12), 3397-415 (1993).